Plant Physiology Preview. Published on January 6, 2015, as DOI:10.1104/pp.114.253682

Running title: An aromatic prenyltransferase metabolon in hop

Corresponding author: Guodong Wang

State Key Laboratory of Plant Genomics and National Center for Plant Gene Research, Institute of Genetics and Developmental Biology, Chinese Academy of Sciences, Beijing 100101, China

Telephone number: 86-10-64806572

E-mail: gdwang@genetics.ac.cn

Research Area: Biochemistry and Metabolism

A heteromeric membrane-bound prenyltransferase complex from *Humulus lupulus* catalyzes three sequential aromatic prenylations in the bitter acid pathway

Haoxun Li[2], Zhaonan Ban[2], Hao Qin, Liya Ma, Andrew J. King and Guodong Wang[*]

State Key Laboratory of Plant Genomics and National Center for Plant Gene Research, Institute of Genetics and Developmental Biology, Chinese Academy of Sciences, Beijing 100101, China (H.L., Z.B., H.Q., L.M., G.W.); Centre for Novel Agricultural Products, Department of Biology, University of York, York YO10 5DD, United Kingdom (A.J.K.); and Graduate School of Chinese Academy of Sciences, Beijing 100049, China (Z.B., L.M.)

One-sentence summary:

A membrane-bound prenyltransferase complex is responsible for all prenylations in the bitter acid pathway in hop glandular trichomes.

1. This work was financially supported by the National Program on Key Basic Research Projects (The 973 Program: 2012CB113900), the National Natural Sciences Foundation of China (Grant 31470387), and the State Key Laboratory of Plant Genomics of China (Grants SKLPG2011B0104 and SKLPG2011A0104) to G.W.

2. These authors contributed equally to this work.

* Corresponding author: Guodong Wang; E-mail: gdwang@genetics.ac.cn

ABSTRACT

Bitter acids (α-type and β-type) account for more than 30% of the fresh weight of hop (*Humulus lupulus* L.) glandular trichomes and are well-known for their contribution to the bitter taste of beer. These multi-prenylated chemicals also show diverse biological activities, some of which have potential benefits to human health. The bitter acid biosynthetic pathway has been investigated extensively and the genes for the early steps of bitter acid synthesis have been cloned and functionally characterized. However, little is known about the enzyme(s) that catalyze three sequential prenylation steps in the β-bitter acid pathway. Here, we employed a yeast system for the functional identification of aromatic prenyltransferase genes (PT). Two PT genes (*HlPT1L* and *HlPT2*) obtained from a hop trichome-specific cDNA library were functionally characterized using this yeast system. Coexpression of codon-optimized *PT1L* and *PT2* in yeast, together with upstream genes, led to the production of bitter acids, but no bitter acids were detected when either of the PT genes was expressed by itself. Step-wise mutation of the Asp-rich motifs in PT1L and PT2 further revealed the prenylation sequence of these two enzymes in β-bitter acid biosynthesis: PT1L only catalyzed the first prenylation step; PT2 catalyzed the two subsequent prenylation steps. A metabolon formed through interactions between PT1L and PT2 was demonstrated using a yeast two hybrid system, reciprocal co-immunoprecipitation, and *in vitro* biochemical assays. These results provide direct evidence of the involvement of a functional metabolon of membrane-bound prenyltransferases in bitter acid biosynthesis in hop.

INTRODUCTION

Hop (*Humulus lupulus* L. Cannabaceae) is an important commodity in the beer brewing industry, mostly due to its high content of bitter acids (a mixture of humulone and lupulone derivatives) and prenylated flavonoids in the glandular trichomes of female flowers (Stevens et al., 1998; Stevens and Page, 2004; Wang et al., 2008; Van Cleemput et al., 2009). Recent studies have demonstrated that hop terpenophenolics (a term for both bitter acids and prenylated flavonoids) exhibit diverse biological activities and have a high potential for use in drug development (Goto et al., 2005; Zanoli and Zavatti, 2008; Saugspier et al., 2012). For these reasons, a combination of large-scale trichome-targeted EST sequencing (thus far there are more than 22,000 ESTs deposited in the TrichOME database (http://www.planttrichome.org) and large amount of RNAseq data from different hop tissues (and cultivars) had been deposited in NCBI (http://www.ncbi.nlm.nih.gov/sra?term=humulus%20lupulus)), reverse genetics, and *in vitro* biochemical assays have been employed in the study of terpenophenolic biosynthesis; several key enzymes have been identified and functionally characterized in recent years (Okada et al., 2004; Nagel et al., 2008; Wang et al., 2008; Wang and Dixon, 2009; Dai et al., 2010; Tsurumaru et al., 2012; Xu et al., 2013). Thus far, we know that the precursors for terpenophenolic biosynthesis are derived from amino acid catabolism (Leu, Ile, and Val for bitter acids and Phe for XN (xanthuhomol)) and the DMAPP (dimethylallyl diphosphate) generated from the plastid-localized MEP (2-C-methyl-d-erythritol 4-phosphate) (Fig. 1). The prenylation steps are critical for final product formation in hop trichomes, and include one prenylation for XN, two prenylations for α-acids, and three prenylations for β-acids. It is known that all of these prenylations use DMAPP as the prenyl donor (Fig. 1). The efficiency of prenyltransferase enzymes in hop trichomes is assumed to be very high, as intermediate compounds (e.g. acylphloroglucinol derivatives and naringenin chalcone (NC)) are barely detectable as compared to the very high concentrations of the prenylated products (Nagel et al., 2008; Clark et al., 2013; Xu et al., 2013). In addition to the aforementioned major prenylated chemicals, geranylated chemicals have also been detected in hop tissues, although these occur at lower

concentrations (Stevens et al., 2000).

In plants, the prenylation reactions are catalyzed by aromatic prenyltransferases, which contribute an additional facet to the metabolic diversity in plant specialized metabolism. Unlike the soluble aromatic prenyltransferases from fungi and bacteria, all aromatic prenyltransferases isolated from plants thus far are membrane-bound proteins (Yazaki et al., 2009). In addition to being membrane proteins, these plant aromatic prenyltransferases also share other common characters including plastid localization, divalent ion-dependenency, and relative narrow substrate specificities. The first flavonoid prenyltransferase gene, which catalyzes the prenylation of naringenin at the 8-position, was recently identified from *Sophora flavescens* root (designated as *SfN8DT-1*) (Sasaki et al., 2008). Several plant aromatic prenyltransferase genes were cloned from various plant species using homologous gene cloning strategies (Akashi et al., 2009; Shen et al., 2012; Karamat et al., 2014; Munakata et al., 2014). Likewise, one membrane-bound prenyltransferase gene (*HlPT-1*) was recently cloned from hops (Tsurumaru et al., 2012). Biochemical results showed that HlPT-1 recognized three acylphloroglucinols (phlorisovalerophenone, PIVP; phlorisobutyrophenone, PIBP; phlormethylbutanophenone, PMBP) and NC as substrates. However, HlPT-1 transferred only one DMAPP to these prenyl acceptors, and the enzymatic conversion rate was relatively low (688 ± 29.7 pmol/mg microsomal protein/h) (Tsurumaru et al., 2012). This result suggests that some unknown factors are required for completing bitter acid biosynthesis in hops, particularly the second and the third prenylation steps in the pathway. There has been extensive interest in the large-scale production of these value-added prenylated chemicals, due to their diverse biological activities and use in the brewing industry. However, simply overexpressing known aromatic prenyltranferase genes, either in plant or in microbial hosts, has not yet generated satisfactory results (Sasaki et al., 2009; Koeduka et al., 2011; Sugiyama et al., 2011). Additionally, no PT that catalyzes more than one prenylation reaction has been reported, although multi-prenylated polyketides occur widely in plants (Singh and Bharate, 2006).

Previously, we functionally characterized two branched short-chain fatty acid CoA

ligase genes (*HlCCL2*/*HlCCL4*). We further successfully reconstructed the upstream steps of the bitter acid pathway by co-introducing *HlCCL2*/*HlCCL4* and *HlVPS* (valerophenone synthase) in a yeast system to produce PIVP, PIBP, and PMBP. This yeast system now serves as a bio-platform that can be used to characterize the remaining enzymatic steps in the bitter acid biosynthesis pathway (Xu et al., 2013). Here, we used an optimized yeast system, combined with site-directed mutagenesis, split-ubiqutin membrane yeast two-hybrid (MbY2H), reciprocal co-immunoprecipatation, and *in vitro* biochemical assays to characterize two candidate aromatic prenyltransferase genes (*HlPT1L* and *HlPT2*) from hop trichomes. Our results showed that PT2 physically interacted with PT1L to form a functional hetero-complex that catalyzed the major prenylations in the bitter acid pathway with high efficiency. PT1L catalyzed the first prenylation step and PT2 catalyzed the subsequent two prenylation steps. Identification of a heteromeric membrane-bound prenyltransferase complex in this study provides tools for the metabolic engineering of high-value prenylated natural products using the strategies of synthetic biology.

Results and Discussion

Yeast Strain Selection for Membrane-Bound Aromatic Prenyltransferases

We selected yeast system to characterize the genes involved in bitter acid pathway due to the lack of a hop transformation system, including the transient gene silencing technique (Xu et al., 2013). To test whether *S. cerevisiae* was a suitable host for plant aromatic prenyltransferase, we co-expressed *HlCCL1/HlCCL8* (the coumarate CoA ligase and malonyl CoA ligase that we cloned previously from hops, GenBank accession number JQ740203 and JQ740210 (Xu et al., 2013)), *HlCHS* (chalcone synthase) and *SfN8DT-1* (the first characterized flavonoid prenyltransferase from plants (Sasaki et al., 2008)) together in a wild-type yeast strain (*YPH499*) and fed with 1.0 mM of coumarate. The chemical analysis of the resulting culture medium by LC-MS showed that only tiny amounts of 8-dimethylallyl naringenin (8DN) could be detected (the conversion ratio to

8-DN from the sum of naringenin and NC was 0.33 ± 0.099%, *n* = 3). This suggested that the availability of DMAPP in *YPH499* may be a limiting factor for the prenylation of naringenin by SfN8DT-1. In yeast cells, the DMAPP and IPP generated from the mevalonate pathway are used in the biosynthesis of isoprenoids such as sterols and ubiquinone. To obtain a yeast strain with a larger pool of DMAPP than that of *YPH499*, two engineered yeast strains were tested: AM94 (this strain produces more FPP for sesquiterpene production (Ignea et al., 2011)) and *DD104* (down-regulation of endogenous farnesyl pyrophosphate synthase (*ERG20*) by site-mutation of K197G, which was originally designed for monoterpene production (Fischer et al., 2011)) (Supplemental Fig. S1). When co-expressing the same set of genes that had been introduced into *YPH499*, the bioconversion of 8DN from naringenin and NC in *DD104* increased 44 fold compared to *YPH499* (14.52 ± 1.79% vs. 0.33 ± 0.099%, *n* = 3). No significant difference in 8DN production was observed between *AM94* and *YPH499* (0.46 ± 0.003% vs. 0.33 ± 0.099%, *n* = 3) (Fig. 2). A previous study had shown that the bio-conversion from naringenin to 8DN by SfN8DT-1 ranged from 0.5% to 2.0% in the *W303-1A-Δcoq2* yeast strain (for complete details of the genetic background, see Supplemental Table S1 and Supplemental Fig. S1D) (Sasaki et al., 2009). We thus selected the *DD104* strain for use in our hop prenyltransferase study.

Identification of Aromatic Prenyltransferase Candidates from a Hop Trichome-Specific Database

As previously mentioned, bitter acid and XN biosynthesis occurs predominantly in the glandular trichomes of female hop flowers (Nagel et al., 2008; Xu et al., 2013). Two putative aromatic prenyltransferase genes were identified with BLAST against the hop trichome-specific library in the TrichOME website using SfN8DT-1 as a query, and the full length cDNA of these two putative aromatic prenyltransferase genes were obtained with RACE (rapid amplification of cDNA ends). One candidate gene (encoding a peptide of 414 amino acids, TCHL40971 in the TrichOME database) was found to be 98.5% identical to

the prenyltransferase gene (Genbank accession number AB543053, designated as HlPT-1) cloned by Yazaki's group from a hop cultivar (Kirin II) (Tsurumaru et al., 2010). The sequence difference between these two proteins was probably due to the different hop cultivar (Nugget) we used for cDNA library construction, we thus designated this *HlPT-1* allele as HlPT1-like (*HlPT1L*). Another candidate gene, designated as *HlPT2*, encodes a polypeptide of 408 amino acids (GD252109 and GD245380 in the TrichOME database). HlPT1L and HlPT2 share 47.0% identity to each other at the protein level, and share 24.2% and 22.5% identity to SfN8DT-1, respectively (Supplemental Fig. S2). Both HlPT1L and HlPT2 contain two conserved Asp-rich motifs and plastid signal peptides at N-terminal predicted by TargetP (www.cbs.dtu.dk/services/TargetP/), which we confirmed with GFP experiments (Fig. 3C and Supplemental Fig. S2). Analysis of the peptide sequences using TMHMM Server v2.0 indicated that HlPT1L and HlPT2 have 8 and 9 predicted transmembrane domains, respectively (Fig. 3A). The trichome-specific expression pattern of *HlPT1L* and *HlPT2*, together with their localization in plastids, suggested that both genes are likely involved in bitter acid and XN biosynthesis (Fig. 3B and C). Phylogenetic analysis showed that both HlPT1L and HlPT2 shared a common ancestor with the VTE2-2 (Vitamin E 2-2; HlPT1L and HlPT2 share 43.2% and 40.2% identity to VTE2-2 at the protein level, respectively) enzymes, which are involved in plastoquinone biosynthesis in Arabidopsis (Tian et al., 2007) (Supplemental Fig. S3).

Coexpression of Codon-optimized *PT1L* and *PT2* Led to Bitter Acid Production in Yeast

We initially tested whether the coexpression of *HlPT1L* and *HlPT2* in the *DD104* yeast strain harboring *CCL2/CCL4/VPS* genes led to the production of prenylated acylphloroglucinols. Under shake flask culture conditions, the engineered yeast strain produce mono-prenylated acylphloroglucinol (including mono-dimethylallylated (MD-) and geranylated (G-) acylphloroglucinols; total 1.2 μmol/L/OD), and a trace amount of di-dimethylallylated (DD-) acylphloroglucinol (total 0.2 μmol/L/OD), but no bitter acids (Supplemental Fig. S6). We further tested whether codon optimization of hop PT genes would increase the production of prenylated acylphloroglucinol. The yeast and

Arabidopsis (designed for functional identification of PT genes *in planta*) codon-optimized version of these two hop prenyltransferase genes were synthesized (for the detailed sequences see Figs. S4 and S5). Unexpectedly, the yeast strain harboring the yeast-optimized *PT1L*/*PT2* (designated as *PT1L-Sc* and *PT2-Sc,* respectively; Supplemental Fig. S4) produced even less prenylated acylphloroglucinols than did the yeast strain harboring *HlPT1L*/*HlPT2* of hop origin (Supplemental Fig. S6). However, the yeast strain harboring the Arabidopsis codon-optimized *PT1L*/*PT2* (designated as *PT1L-At* and *PT2-At,* respectively; Supplemental Fig. S5) produced the highest amount of prenylated acylphloroglucinol (total 10.8 µmol/L/OD), including 6.54 µmol/L/OD of MD-acylphloroglucinol, 1.72 µmol/L/OD of geranylated (G-) acylphloroglucinol, 2.17 µmol/L/OD of DD-acylphloroglucinol ,and 0.37 µmol/L/OD total β-acids, after galactose induction for 48 hours (Fig. 4 and Supplemental Fig. S6). Based on these results, we used Arabidopsis codon-optimized *PT1L* and *PT2* for further studies (designated as *PT1L-At* and *PT2-At,* respectively). It is noteworthy to point out that our LC-MS method did not distinguish PIVP and PMBP (which are isomeric) and their corresponding derivatives, with the exception of lupulone (a PIVP derivative) and adlupulone (a PMBP derivative). We thus use the term “PIVP” to represent the mixture of PIVP and PMBP for convenience. We further tested the effect of *PT1L-At* alone or *PT2-At* alone on the production of prenylated acylphloroglucinols. The *PT1L-At* alone strain produced 4.38 µmol/L/OD of acylphloroglucinol, 0.11 µmol/L/OD of MD-acylphloroglucinol, and 0.026 µmol/L/OD of G-acylphloroglucinol. No prenylated compounds were produced by the strain harboring only *PT2-At* or the control strain lacking the PT genes (Fig. 4). The retention times and mass spectraof PIBP, PIVP, MD-PIBP, and PIVP were identical to those of authenbtic standards (here we used the chemical extract of hops trichome as standards for cohumulone, humulone, and adhumulone); the chemical structures of G-PIBP (geranylated phlorisobutyrophenone), G-PIVP geranylated phlorisovalerophenone, DD-PIVP (di-dimethylallylated phlorisovalerophenone, also known as 4-deoxycohumulone), and DD-PIBP (di-dimethylallylated phlorisobutyrophenone, also known as 4-deoxycohumulone) were tentatively elucidated from their mass spectra (the mass spectra of standards and other compounds are shown in Supplemental Fig. S7).

It has been demonstrated that the *N*-terminal signal peptide somehow inhibits the enzymatic activity of isoflavonoid-specific prenyltransferase (LaPT1) from white lupin (*Lupinus albus*) (Shen et al., 2012). We thus coexpressed truncated *PT1L-At* (with an 86 amino acid deletion from the start codon, based on the signal peptide prediction by TargetP; truncated *PT1L-At* was renamed as *PT1L-T*) and truncated *PT2-At* (with 83 amino acid deletion from the start codon; the truncated *PT2-At* was renamed as *PT2-T*) to test the effect of these signal peptide on the activity of hop prenyltransferase proteins. The resulting yeast produced much higher amounts of bitter acids than did the respective yeast strains harboring full-length *PT1L-At* and *PT2-At* (0.37 μmol/L/OD total β-acids): 2.18 μmol/L/OD total β-acids, after galactose induction for 48 hours (Fig. 4). Unlike the acylphloroglucinols, most of which were secreted into culture medium, > 70% of the prenylated acylphloroglucinols remained inside the yeast cells (Supplemental Fig. S8). No α-acids could be detected in any of the tested yeast strains, indicating that there is an additional enzymatic reaction that is required for the final oxidation step that converts DD-acylphloroglucinols into α-acids.

Different Prenylation Steps Catalyzed by PT1L and PT2 in the Bitter Acid Pathway

Although bitter acids were produced when *PT1L-At* and *PT2-At* were coexpressed together, the roles of PT1L and PT2 in the bitter acid pathway has not been clearly defined. To address this question, we mutated the Asp in Asp-rich motifs (DXXXD or DXXD; X, any amino acid) in PT1L and PT2 to Ala (AXXXA or AXXA; Fig. 5A) and coexpressed one normal PT gene and a mutated PT gene in DD104 yeast harboring *CCL2*/*CCL4*/*VPS.* Previous studies had shown the critical role of the Asp-rich motif for aromatic prenyltransferase activity. Thus, mutation in Asp-rich motif would very likely lead to inactive aromatic prenyltransferases (Ohara et al., 2009; Cheng and Li, 2014). The yeast strain harboring mutated *PT1L-At* and wild-type *PT2-At* did not produce any prenylated products, which revealed that PT1L is responsible for at least the first prenylation step in the bitter acid pathway (this result is consistent with a previous report (Tsurumaru et al., 2012)). Wild-type PT2 did not recognize PIVP/PIBP as a substrate.

Interestingly, the strain harboring wild-type *PT1L-At* and mutated *PT2-At* produced higher amounts mono-prenylated compounds than did the strain harboring *PT1L-At* alone, implying that the inactive PT2 protein, like its wild-type isoform, increases the prenylation efficiency of PT1L (Fig. 5). Meanwhile, no di- or tri- prenylated compounds were produced by the strain harboring wild-type *PT1L-At* and mutated *PT2-At*, suggesting that PT2 is a functional protein that is responsible for the second and third prenylation steps in the β-acids pathway.

HlPT1L Physically Interacts with HlPT2

Higher levels of mono-prenylated compounds were observed when *PT1L-At* and *PTL2-At* were co-expressed, no matter whether they were wild-type or mutated forms, than when expressing *PT1L-At* alone (Fig. 4 and 5). This finding drove us to hypothesize that PT2 may interact with PT1L to form a complex that enables efficient prenyltransferase activity. We thus used a split-ubiquitin MbY2H to test this hypothesis. The results showed that PT2 was able to form a homomer with itself or form a heteromer with PT1L; this result was further confirmed with positive β-galactosidase assays (Fig. 6A). The lack of growth in the negative controls (pDL2-Nx and pDL2-xN are empty vectors) indicated that the detected interactions between PT1L and PT2 were not false positives (Fig. 6A). To further confirm the interaction between PT1L and PT2, we performed co-immunoprecipitation experiments. N-terminal His-tagged *PT1L-T* and N-terminal HA-tagged *PT2-T* were coexpressed in yeast. The results showed that PT2 recombinant protein could be coimmunoprecipitated when the lysates of transformed cells were incubated with an anti-His antibody. The anti-HA antibody could also be coimmunoprecipitated with His-tagged PT1L recombinant protein. However, no interactions between His-tagged PT1L-T and HA-tag (as a negative control) or HA-tagged PT2-T and His-tag (as a negative control) could be detected (Fig. 6B). Together, these results support the hypothesis that HlPT1L/HlPT2 forms and functions as a complex in yeast membranes.

Biochemical Characterization of the Heteromeric Prenyltransferase Complex

To better understand the effect of the heteromeric prenyltransferase complex on the efficiency of prenylation, kinetic analyses of the activities of prenyltransferase complex were carried out. Consistent with the data in yeast, microsomes containing full length PT1L had very weak activity for PIBP and PIVP *in vitro* (too low to be suitable for K_m determination) (Supplemental Fig. S9). The truncated PT1L showed much higher activity to PIBP and PIVP compared to that of the full length PT1L protein (Table 1). Microsomes containing full length PT1L and mutated full length PT2 had 7-10 higher prenyltransferase activity toward PIVP, PIBP, DMAPP, and GPP than did truncated PT1L alone, though these had similar K_m values (Table 1). These results revealed that physical interaction with PT2 increased the turnover rate of PT1L, without changing the affinity of PT1L to substrates. However, the much higher efficiency of PT1L toward GPP than to DMAPP is not consistent with the fact that the dimethylallylated chemicals accumulate to much higher levels than the geranylated chemicals in hops trichomes (Fig. 4; (Stevens and Page, 2004; Xu et al., 2013)). Likely, most of the GPP was consumed by myrcene synthase for monoterpenoid biosynthesis (HlMTS1; (Wang et al., 2008)), not by the prenyltransferase complex for bitter acid production in hops trichomes. It is noteworthy that in our test conditions truncated PT1L (Arabidopsis codon-optimized) also exhibited activity toward NC to form desmethylxanthohumol, albeit at a much lower level (3.4 ± 0.35%, n = 3) as compared to that of PIVP (Fig. S11). This activity was also detected in a previous report (Tsurumaru et al., 2012).

As mentioned above, PT2 catalyzed the last two prenylation steps in the β-bitter acid pathway in yeast cells. The yeast microsomes containing the combination of truncated HlPT1L and truncated HlPT2 (PT1L-T/PT2-T) proteins catalyzed PIVP and DMAPP to form DD-PIVP in vitro, and no lupulone could be found (Fig. S10H). However, prepared yeast microsomes containing the PT2 protein did not further prenylate MD-PIVP (mono-dimethylallylated-phlorisovalerophenone) *in vitro*, regardless of whether PT2 was present singly or together with PT1L, or if PT2 was full-length or truncated (Supplemental Fig. S10B-J). One plausible explanation for this is that a metabolon is formed by PT1L and PT2 and this complex is essential for PT2 enzymatic function. In this scenario, exogenously supplied “intermediate” (MD- acylphloroglucinol in this case) may not be able

to access the enzyme active sites in the metabolon (Winkel, 2004).

Conclusions

Two major conclusions can be drawn from our study. First, we functionally characterized a complex of two aromatic prenyltransferases that catalyzed three sequential prenylation steps in the bitter acid pathway. Biochemical data, together with the results from the yeast two hybrid and the reciprocal co-immunoprecipitation experiments, further supported the hypothesis that a metabolon formed by HlPT1 and HlPT2 in hop glandular trichomes. The aromatic prenyltransferase metabolon demonstrated here, together with the high trichome-specific expression level of the genes involved in the bitter acid pathway (*HlCCL2/4*, *HlVPS* and *HlPT1L/2*), is responsible for the high efficiency of bitter acid biosynthesis in hop trichomes (Okada et al., 2004; Xu et al., 2013). Second, we successfully reconstructed the entire β-bitter acid pathway in a yeast system. Under flask-shake conditions, the engineered yeast produced up to 2.18 μmol/L/OD total β-acids, and it should be possible to further increase bitter acid production by using a combination of strategies from synthetic biology and optimized fermentation conditions (Keasling, 2010; Zhou et al., 2014). The engineered strains in the present study also provide a starting point for the functional identification of other components involved in the bitter acid pathway. Among these, the elucidation of the enzyme responsible for the last oxidation step in the α-bitter acid pathway has the high priority due to its critical role in flavoring beer (Caballero et al., 2012). Several P450s and monooxygenase genes have been identified from the TrichOME database, together with the fact that DD-acylphloroglucinol (the proposed precursor for the reaction) is produced in our engineered yeast, hold promise for the completion of the whole jigsaw puzzle of the complete bitter acid pathway.

MATERIALS AND METHODS

Plant materials, RNA analysis, and Chemicals

The growth of *Humulus lupulus* cv. Nugget, RNA isolation and cDNA preparation from hop tissues, and quantitative real-time PCR were performed as described previously (Wang et al., 2008). The codon-optimized sequences of *PT1L* and *PT2* were generated using the JCat tool (http://www.jcat.de/) (Grote et al., 2005) and synthesized by TaKaRa Bio (China).

All chemicals used in this study were purchased from Sigma-Aldrich (USA) except PIBP/PIVP and their mono-prenylated derivatives, which were synthesized as described previously (George et al., 2010). The purity and concentration of these chemicals were determined using UHPLC-MS and NMR (Supplemental Table S3).

Hop Prenyltransferase Gene Isolation and *In Vitro* Mutagenesis

To obtain the full length sequences of *PT1L* and *PT2* from hop trichomes, 3' RACE was performed with a SMART RACE cDNA Amplification Kit (USA) following the manufacturer's instructions. The open reading frames of *PT1L* and *PT2* obtained by RT-PCR were subcloned into the pGEM®-T Easy vector (Promega, Madison, WI, USA) and verified by sequencing of at least five independent clones (see Supplemental Table S2 for primer information). Nucleotide sequences of *HlPT1L* and *HlPT2* can be found in the GenBank database under accession numbers KM222441 and KM222442, respectively.

The Asp in the conserved Asp-rich motifs in *PT1L* (NQIY**D**^{183}LES**D**^{187} and K**D**^{310}VP**D**^{313}VEGD) and *PT2* (NQIF**D**^{174}MDI**D**^{178} and K**D**^{302}LS**D**^{305}INGD) were mutated to Ala using a previously described PCR-mediated method (Ho et al., 1989). The primers used are detailed in Supplemental Table S2.

Reconstitution of the Bitter Acid Pathway in Yeast and Analysis of Products

HlVPS (GenBank accession number AB015430) was subcloned into the pESC-HIS vector

(Agilent Technologies, USA). The two *HlCCL* genes were subcloned into the pESC-LEU vector (CCl2/4 for bitter acid pathway; GenBank accession number JQ740204 and JQ740206), the *PT1L* and *PT2* (either wild-type or mutated copy) were inserted into the pESC-URA vector singly or together (see Supplemental Table S2 for primer information). The different combinations of three constructs (either empty vector or the construct with inserts) were co-transformed into the appropriate yeast strain using a high efficiency lithium acetate transformation protocol (Gietz and Schiestl, 2007). The resulting positive yeast clones, after being verified by PCR, were cultured in 30 mL of SD dropout medium (-Leu, -His, -Ura) with D-glucose as the carbon source, for two days. Then the yeast cells were harvested and resuspended into SG dropout medium (-Leu, -His, -Ura) with 2% galactose. After induction for an appropriate period, 5 mL aliquots of the cultures were lysed by sonication after measuring cell density, and subsequently extracted with 5 mL of ethyl acetate (10 μM naringenin was added as an internal standard). Extracts were dried under a stream of nitrogen and subsequently dissolved in 60% methanol for LC-MS analysis (1290 liquid chromatograph coupled to a 6550 qTOF mass spectrometer, Agilent Technologies, USA). 2 μL of sample was loaded on HPLC column (ZORBAX Extend-C18, 2.1x50 mm, 1.8-Micron, Agilent) run at a flow rate of 0.4 mL/min. The gradient (solvent A, 0.05% formic acid and 5 mM ammonium formate in 10% acetonitrile; solvent B, 0.05% formic acid and 5 mM ammonium formate in 90% acetonitrile) program was set as follows, at a flow of 0.4 mL/min: 0 to 10 min, a linear gradient from 20 to 90% of B; 10 to 12 min, 90% of B. MS spectra were acquired in positive-ion mode. The operating parameters were set as follows: capillary voltage, 4000 V; nebulizer pressure, 20 psig; drying gas flow rate, 13 L/min; gas temperature, 225 °C; sheath gas flow, 12 L/min; sheath gas temperature, 350°C; fragmentor, 365 V. The content of prenylated compounds in the samples was quantified based on a standard curve prepared with PIVP or PIBP.

Split-Ubiquitin MbY2H Assays

The membrane-bound protein Y2H assays were performed with a DUAL membrane kit following the manufacturer's instructions (Dualsystems Biotech AG, Switzerland). The primers used are listed in Supplemental Table S2.

Co-immunoprecipitation Assays of HlPT1L and HlPT2

N-terminal His-tagged *PT1L-T* (+1 to +258 bp from ATG was removed; designated as 6xHis:HlPT1L-T) and N-terminal HA-tagged *PT2-T* (+1 to +249 bp from ATG was removed; designated as *HA:PT2-T*) were subcloned into the pESC-LEU and the pESC-HIS vectors, respectively. The correct plasmids, confirmed by sequencing, were co-transformed into DSY-1 yeast cells. The pESC-LEU and pESC-HIS were also modified using a PCR-mediated method for expressing His-tag or HA-tag in yeast cells, respecitvely (see Supplemental Table S2 for primer information). The resulting plasmids, renamed as His-pESC-LEU or HA-pESC-HIS, were used as negative controls. The transformed yeast cells were pre-cultured in synthetic dropout medium containing 2% glucose to an OD_{600} value greater than 2.0, then diluted to OD_{600} = 0.4 and cultivated with 2% (w/v) galactose until the OD_{600} value reached 1.0. 400 mL cultures of yeast cells were harvested and disrupted with glass beads with a Mini-Bead-Beater (Biospec Products, USA) in an extraction buffer (2 mL/g cells) containing 50 mM Tris-HCl pH 7.5, 1 mM EDTA, 1% Triton X-100, 1 mM PMSF, 1 µg/mL leupeptin, and 1 µg/mL pepstatin. Glass beads and cell debris were removed by 2 rounds of centrifugation at 12,000 x *g* for 15 min. The supernatant was incubated with the first antibody (anti-His or anti-HA) at 4°C overnight with shaking, followed by incubation with protein G agarose beads for an additional 4 h. The beads were washed twice with extraction buffer supplemented with 150 mM NaCl and then resuspended in SDS-PAGE sample buffer. The immunoprecipitated proteins were separated by 15% SDS-PAGE, transferred to a PVDF membrane, and blotted with appropriate antibodies (anti-His or anti-HA).

In Vitro Prenyltransferase Assay

Yeast microsome preparationw were carried out as described by Pompon *et al.* (Pompon et al., 1996). The microsomal proteins were directly used for prenyltransferase assays after quantification by Bradford assay. The standard prenyltransferase assay reaction contained 1 mM dithiothreitol, 10 mM Tris-HCl (pH 7.0), 10 mM $MgCl_2$, 30 mM NaF using

as a phosphatase inhibitor, 100 µM prenyl donor chemicals, and 100 µM DMAPP. The reaction mixtures were incubated in a total volume of 250 µL at 30°C. The enzymatic reaction mixtures were extracted twice with 250 µL of ethyl acetate. The organic phases of the extracts were combined and dried under nitrogen gas. Extracts were then dissolved in 250 µL of 40% methanol, and 1 µl of the resulting solution was analyzed with LC-qTOF-MS. For the determination of the apparent K_m value of different substrates, 100 µM prenyl donor was added in the standard PT reactions (200 µL volume) containing a series of concentrations of prenyl acceptors, and *vice versa*. The enzymatic products were extracted and quantified using aforementioned protocol. The apparent K_m data were calculated by using Hanes plots (Hyper32, version 1.0.0).

ACKNOWLEDGEMENTS

We thank Dr. Francis Karst at the University of Strasbourg, France, for providing the *DD104* yeast strain, Dr. Antonios Makris at the Mediterranean Agronomic Institute of Chania, Greece, for providing the *AM94* yeast strain, Dr. Kazufumi Yazaki at Kyoto University, Japan, for providing the *W303-1A-Δcoq2* yeast strain and the *SfN8DT* clone (in pDR196 vector), and Dr. Ben Moulton at York University, U.K., for his help with the chemical synthesis of PIBP and PIVP.

LITERATURE CITED

Akashi T, Sasaki K, Aoki T, Ayabe S-i, Yazaki K (2009) Molecular cloning and characterization of a cDNA for pterocarpan 4-dimethylallyltransferase catalyzing the key prenylation step in the biosynthesis of glyceollin, a soybean phytoalexin. Plant Physiol **149:** 683-693

Caballero I, Blanco CA, Porras M (2012) Iso-alpha-acids, bitterness and loss of beer quality during storage. Trends Food Sci Tech **26:** 21-30

Cheng W, Li W (2014) Structural insights into ubiquinone biosynthesis in membranes. Science **343:** 878-881

Clark SM, Vaitheeswaran V, Ambrose SJ, Purves RW, Page JE (2013) Transcriptome analysis of bitter acid biosynthesis and precursor pathways in hop (*Humulus lupulus*). BMC Plant Biol **13:** 12

Dai X, Wang G, Yang DS, Tang Y, Broun P, Marks MD, Sumner LW, Dixon RA, Zhao PX (2010) TrichOME: a comparative omics database for plant trichomes. Plant Physiol **152:** 44-54

Fischer MJ, Meyer S, Claudel P, Bergdoll M, Karst F (2011) Metabolic engineering of monoterpene synthesis in yeast. Biotechnol Bioeng **108:** 1883-1892

George JH, Hesse MD, Baldwin JE, Adlington RM (2010) Biomimetic synthesis of polycyclic polyprenylated acylphloroglucinol natural products isolated from *Hypericum papuanum*. Org Lett **12:** 3532-3535

Gietz RD, Schiestl RH (2007) High-efficiency yeast transformation using the LiAc/SS carrier DNA/PEG method. Nat Protoc **2:** 31-34

Goto K, Asai T, Hara S, Namatame I, Tomoda H, Ikemoto M, Oku N (2005) Enhanced antitumor activity of xanthohumol, a diacylglycerol acyltransferase inhibitor, under hypoxia. Cancer Lett **219:** 215-222

Grote A, Hiller K, Scheer M, Munch R, Nortemann B, Hempel DC, Jahn D (2005) JCat: a novel tool to adapt codon usage of a target gene to its potential expression host. Nucleic Acids Res **33:** W526-W531

Ho SN, Hunt HD, Horton RM, Pullen JK, Pease LR (1989) Site-directed mutagenesis by overlap extension using the polymerase chain reaction. Gene **77:** 51-59

Ignea C, Cvetkovic I, Loupassaki S, Kefalas P, Johnson CB, Kampranis SC, Makris AM (2011) Improving yeast strains using recyclable integration cassettes, for the production of plant terpenoids. Microb Cell Fact **10:** 1-18

Karamat F, Olry A, Munakata R, Koeduka T, Sugiyama A, Paris C, Hehn A, Bourgaud F, Yazaki K (2014) A coumarin-specific prenyltransferase catalyzes the crucial biosynthetic reaction for furanocoumarin formation in parsley. Plant J **77:** 627-638

Keasling JD (2010) Manufacturing molecules through metabolic engineering. Science **330:** 1355-1358

Koeduka T, Shitan N, Kumano T, Sasaki K, Sugiyama A, Linley P, Kawasaki T, Ezura H, Kuzuyama T, Yazaki K (2011) Production of prenylated flavonoids in tomato fruits expressing a prenyltransferase gene from *Streptomyces coelicolor* A3 (2). Plant Biology **13:** 411-415

Munakata R, Inoue T, Koeduka T, Karamat F, Olry A, Sugiyama A, Takanashi K, Dugrand A, Froelicher Y, Tanaka R, Uto Y, Hori H, Azuma J-I, Hehn A, Bourgaud F, Yazaki K (2014) Molecular cloning and characterization of a geranyl diphosphate-specific aromatic prenyltransferase from lemon. Plant Physiol **166:** 80-90

Nagel J, Culley LK, Lu YP, Liu EW, Matthews PD, Stevens JF, Page JE (2008) EST analysis of hop glandular trichomes identifies an *O*-methyltransferase that catalyzes the biosynthesis of xanthohumol. Plant Cell **20:** 186-200

Ohara K, Muroya A, Fukushima N, Yazaki K (2009) Functional characterization of LePGT1, a membrane-bound prenyltransferase involved in the geranylation of p-hydroxybenzoic acid. Biochem J **421:** 231-241

Okada Y, Sano Y, Kaneko T, Abe I, Noguchi H, Ito K (2004) Enzymatic reactions by five chalcone synthase homologs from hop (*Humulus lupulus* L). Biosci Biotech Bioch **68:** 1142-1145

Pompon D, Louerat B, Bronine A, Urban P (1996) Yeast expression of animal and plant P450s in optimized redox environments. Method Enzymol **272:** 51-64

Sasaki K, Mito K, Ohara K, Yamamoto H, Yazaki K (2008) Cloning and characterization

of naringenin 8-prenyltransferase, a flavonoid-specific prenyltransferase of *Sophora flavescens*. Plant Physiol **146:** 1075-1084

Sasaki K, Tsurumaru Y, Yazaki K (2009) Prenylation of flavonoids by biotransformation of yeast expressing plant membrane-bound prenyltransferase *SfN8DT-1*. Biosci Biotech Bioch **73:** 759-761

Saugspier M, Dorn C, Thasler WE, Gehrig M, Heilmann J, Hellerbrand C (2012) Hop bitter acids exhibit anti-fibrogenic effects on hepatic stellate cells *in vitro*. Exp Mol Pathol **92:** 222-228

Shen G, Huhman D, Lei Z, Snyder J, Sumner LW, Dixon RA (2012) Characterization of an isoflavonoid-specific prenyltransferase from *Lupinus albus*. Plant Physiol **159:** 70-80

Singh IP, Bharate SB (2006) Phloroglucinol compounds of natural origin. Nat Prod Rep **23:** 558-591

Stevens JF, Miranda CL, Buhler DR, Deinzer ML (1998) Chemistry and biology of hop flavonoids. J Am Soc Brew Chem **56:** 136-145

Stevens JF, Page JE (2004) Xanthohumol and related prenylflavonoids from hops and beer: to your good health! Phytochemistry **65:** 1317-1330

Stevens JF, Taylor AW, Nickerson GB, Ivancic M, Henning J, Haunold A, Deinzer ML (2000) Prenylflavonoid variation in *Humulus lupulus*: distribution and taxonomic significance of xanthogalenol and 4'-*O*-methylxanthohumol. Phytochemistry **53:** 759-775

Sugiyama A, Linley PJ, Sasaki K, Kumano T, Yamamoto H, Shitan N, Ohara K, Takanashi K, Harada E, Hasegawa H (2011) Metabolic engineering for the production of prenylated polyphenols in transgenic legume plants using bacterial and plant prenyltransferases. Metab Eng **13:** 629-637

Tian L, DellaPenna D, Dixon RA (2007) The *pds2* mutation is a lesion in the Arabidopsis homogentisate solanesyltransferase gene involved in plastoquinone biosynthesis. Planta **226:** 1067-1073

Tsurumaru Y, Sasaki K, Miyawaki T, Momma T, Umemoto N, Yazaki K (2010) An aromatic prenyltransferase-like gene *HlPT-1* preferentially expressed in lupulin

glands of hop. Plant Biotechnol-NAR **27:** 199-204

Tsurumaru Y, Sasaki K, Miyawaki T, Uto Y, Momma T, Umemoto N, Momose M, Yazaki K (2012) HlPT-1, a membrane-bound prenyltransferase responsible for the biosynthesis of bitter acids in hops. Biochem Biophys Res Commun **417:** 393-398

Van Cleemput M, Cattoor K, De Bosscher K, Haegeman G, De Keukeleire D, Heyerick A (2009) Hop (*Humulus lupulus*)-derived bitter acids as multipotent bioactive compounds. J Nat Prod **72:** 1220-1230

Wang G, Dixon RA (2009) Heterodimeric geranyl(geranyl)diphosphate synthase from hop (*Humulus lupulus*) and the evolution of monoterpene biosynthesis. Proc Natl Acad Sci USA **106:** 9914-9919

Wang G, Tian L, Aziz N, Broun P, Dai XB, He J, King A, Zhao PX, Dixon RA (2008) Terpene biosynthesis in glandular trichomes of hop. Plant Physiol **148:** 1254-1266

Winkel BSJ (2004) Metabolic channeling in plants. Annu Rev Plant Biol **55:** 85-107

Xu H, Zhang F, Liu B, Huhman DV, Sumner LW, Dixon RA, Wang G (2013) Characterization of the formation of branched short-chain fatty acid:CoAs for bitter acid biosynthesis in hop glandular trichomes. Mol Plant **6:** 1301-1317

Yazaki K, Sasaki K, Tsurumaru Y (2009) Prenylation of aromatic compounds, a key diversification of plant secondary metabolites. Phytochemistry **70:** 1739-1745

Zanoli P, Zavatti M (2008) Pharmacognostic and pharmacological profile of *Humulus lupulus* L. J Ethnopharmaco **116:** 383-396

Zhou J, Du G, Chen J (2014) Novel fermentation processes for manufacturing plant natural products. Curr Opin Biotech **25:** 17-23

Figure Legends

Figure 1. The proposed biosynthetic pathway for bitter acids and xanthohumol in hop glandular trichomes. The major prenylation steps in the pathway are highlighted in red and possible R-group in acylphloroglucinols, DD-acylphloroglucinols and bitter acids are isobutyryl, isopropyl, and butan-2-yl groups. CCL, carboxyl CoA ligase; CHS, chalcone synthase; DMAPP, dimethylallyl diphosphate; DD-acylphloroglucinols, di-dimethylallylated acylphloroglucinol; MT, methyltransferase; PT, prenyltransferase; VPS, valerophenone synthase.

Figure 2. *In vivo* production of 8DN in various yeast strains. (A) Chemical profiling of different yeast strains by LC-ESI-QQQ/MS. 8DN, 8-dimethylallyl naringenin (RT: 3.54 min, MRM transition: *m/z* 339→119); N, naringenin (RT: 1.73 min, MRM mode: *m/z* 271→119); NC, naringenin chalcone (RT: 1.60 min, MRM mode: *m/z* 271→151). (B) Bioconversion ratio of 8DN from the sum of N and NC in different yeast strains. All experiments were performed in triplicate.

Figure 3. Characterization of HlPT1L and HlPT2 in hop. (A) Membrane topology diagram of HlPT1L and HlPT2. The transmembrane domains and the Asp-rich motifs are highlighted in gray and red, respectively. (B) qRT-PCR analysis of two PT genes in different tissues and different development stages of cones and trichomes. Transcript levels are expressed relative to the GAPDH gene (n = 3). WAF, Weeks after flowering. (C) Subcellular localizations of HlPT1L (the first 86 amino acids at the *N* terminus) and HlPT2 (the first 83 amino acids at the N terminus) in Arabidopsis leaf-mesophyll protoplasts, as revealed by laser confocal microscopy. Chloroplasts are revealed by red chlorophyll autofluorescence. SP, signal peptide; Scale bars = 10 μm.

Figure 4. *In vivo* production of prenylated chemicals in yeast cells co-expressing *HlCCL2*, *HlCCL4*, *HlVPS,* and different hop aromatic prenyltransferase genes. (A) Chromatogram of selected ions of m/z 197.0808 for PIBP, m/z 211.0965 for PIVP, m/z 265.1434 for

MD-PIBP, m/z 279.1591 for MD-PIVP, m/z 333.206 for DD-PIBP and G-PIBP, m/z 347.2217 for DD-PIVP and G-PIVP, m/z 401.2715 for colupulone, and m/z 415.2863 for lupulone and adlupulone, all with a mass accuracy in the 20 ppm range. Some regions of these chromatograms have been rescaled to allow easier visualization. (B) Production of different chemicals by yeast strains harboring no *PT* gene (control), *PT1L*, *PT2, PT1L*/*PT2* or *PT1L-T*/*PT2-T* (the combination of truncated *HlPT1L* and *HlPT2*). Data are means ± SD for at least three independent clones. All PT genes used in this experiment were Arabidopsis codon-optimized sequences.

Figure 5. Effects of the Asp-rich motif on bitter acid production in engineered yeast strains. (A) Sequence comparisons of wild-type (control) and mutant PT1L/PT2. Only the Asp-rich motifs are shown, and the mutated amino acids are in bold and italics. (B) Production of different compounds by yeast strains harboring wild-type and mutated *PT1L*/*PT2* pairs. Data are means ± SD for at least three independent clones. All PT genes used in this experiment were Arabidopsis codon-optimized sequences.

Figure 6. Direct interaction between PT1L and PT2 in yeast membranes. (A) Split-ubiquitin assays for PT1L and PT2 protein interactions. The different transformed yeast cells were serially diluted and spotted onto growth media (SD/Trp^-/Leu^-) and selection media (SD/Trp^-/Leu^-/His^-), both supplemented with 50 mM 3-AT (3-amino-1,2,4-triazole). The positive interaction between PT1L and PT2 was confirmed by filter assay for detection of X-galactosidase activity. (B) Reciprocal co-immunoprecipitation of His-tagged truncated PT1L and HA-tagged truncated PT2 in yeast cells using HA- and His- antibodies. Total protein extracts from transformed yeast strains harboring truncated *PT1L-At* and *PT2-At* alone or together, were incubated with anti-His or anti-HA antibodies, and the immunoprecipitates were separated by SDS-PAGE and subjected to immunoblot analysis using anti-HA or anti-His antibodies. The His-pESC-LEU and HA-pESC-HIS (producing the His-tag or HA-tag peptide only in yeast cells) were used as negative controls. Ab, antibody.

Table 1. Kinetic parameters for PT1L, PT1L-T, and PT1L/PT2 (M3). All PT genes used in this experiment were Arabidopsis codon-optimized sequences. The data are presented as means ± SD (n = 3).

Enzyme	Substrate	K_m (μM)	V_{max} (μmol/mg microsomal protein/min)
PT1L	PIVP[a]	N.D.	N.D.
	PIBP[a]	N.D.	N.D.
	DMAPP[b]	N.D.	N.D.
	GPP[b]	N.D.	N.D.
PT1L-T	PIVP[a]	1.36 ± 0.43	1.08 ± 0.19
	PIBP[a]	5.1 ± 0.81	0.41 ± 0.03
	DMAPP[b]	43.52 ± 3.7	0.47 ± 0.04
	GPP[b]	5.70 ± 1.07	0.69 ± 0.02
PT1L/PT2 (M3)	PIVP[a]	3.39 ± 0.73	7.96 ± 1.77
	PIBP[a]	6.68 ± 1.08	3.06 ± 0.38
	DMAPP[b]	43.64 ± 23.35	4.75 ± 1.94
	GPP[b]	6.18 ± 1.37	5.36 ± 0.82

[a] 100 μM DMAPP used as prenyl donor.

[b] 100 μM PIVP used as prenyl acceptor.

N.D. not determined due to the low PT activity.

Supplemental Data

Supplemental Figure S1. The prenyl diphospahte pathway in different yeast strains *YPH499* (A), *DD104* (B), *AM94* (C), and *W303-1A-Δcoq2* (D) used in this study.

Supplemental Figure S2. Alignment of HlPT1L and HlPT2 with SfN8DT-1 (cloned from *S. flavescens,* GenBank number AB325579).

Supplemental Figure S3. Phylogenetic analyses of HlPT1L, HlPT2, and their homologs from other plant lineages.

Supplemental Figure S4. Nucleotide Alignment of *HlPT1L*, *PT1L-At,* and *PT1L-Sc*.

Supplemental Figure S5. Nucleotide Alignment of *HlPT2*, *PT2-At,* and *PT2-Sc*.

Supplemental Figure S6. Production of acylphloroglucinols and prenylated acylphloroglucinols in yeast strains harboring different codon-optimized *PT1L/PT2* pairs.

Supplemental Figure S7. ESI-MS (in positive mode) spectra of the compounds produced in an engineered yeast strain harboring CCL2/CCL4/VPS/HlPT1L/HlPT2 or hop glandular trichomes.

Supplemental Figure S8. Distribution of acylphloroglucinols (AP) and prenylated acylphloroglucinols produced by a yeast strain harboring *CCL2*/*CCL4*/*VPS*/*PT1L-T*/*PT2-T* in cells (Intra) and in the culture medium (Extra).

Supplemental Figure S9. LC-q-TOF/MS analysis of products generated by yeast microsomes containing different prenyltransferase proteins, using PIVP or PIBP as substrate.

Supplemental Figure S10. LC-q-TOF/MS analysis of enzymatic products generated by yeast microsomes containing different prenyltransferase proteins, using mono-prenylated PIVP as a substrate.

Supplemental Figure S11. Substrate specificity of yeast microsome harboring truncated HlPT1L.

Supplemental Table S1. Yeast strains and plasmids used in this study.

Supplemental Table S2. Primers used in the present study.

Supplemental Table S3. ^{1}H NMR and ^{13}C NMR signal assignment for PIBP, PIVP, MD-PIBP and MD-PIVP.

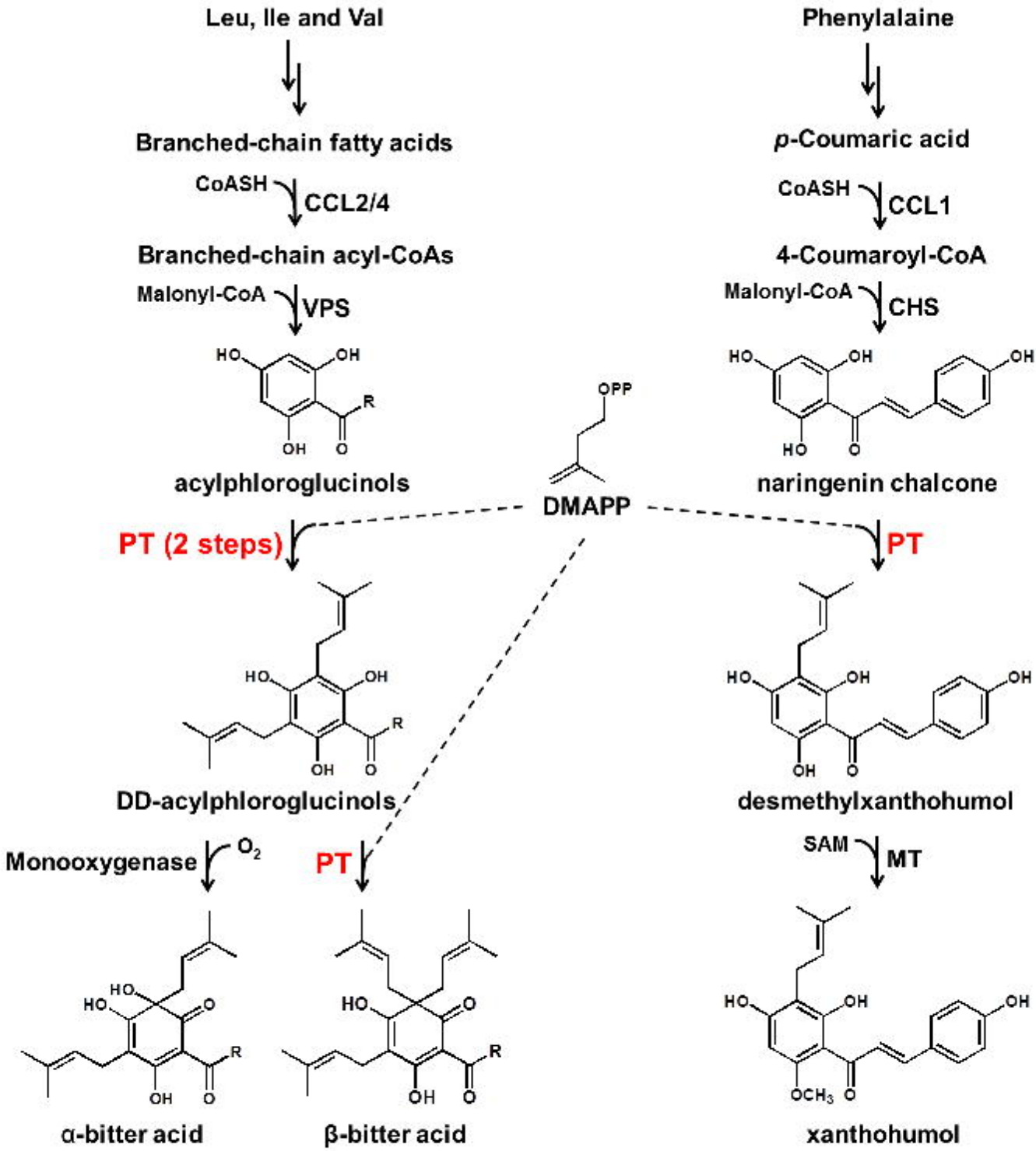

Figure 1. The proposed biosynthetic pathway for bitter acids and xanthohumol in hop glandular trichomes. The major prenylation steps in the pathway are highlighted in red and possible R-group in acylphloroglucinols, DD-acylphloroglucinols and bitter acids are isobutyryl, isopropyl, and butan-2-yl groups. CCL, carboxyl CoA ligase; CHS, chalcone synthase; DMAPP, dimethylallyl diphosphate; DD-acylphloroglucinols, di-dimethylallylated acylphloroglucinol; MT, methyltransferase; PT, prenyltransferase; VPS, valerophenone synthase.

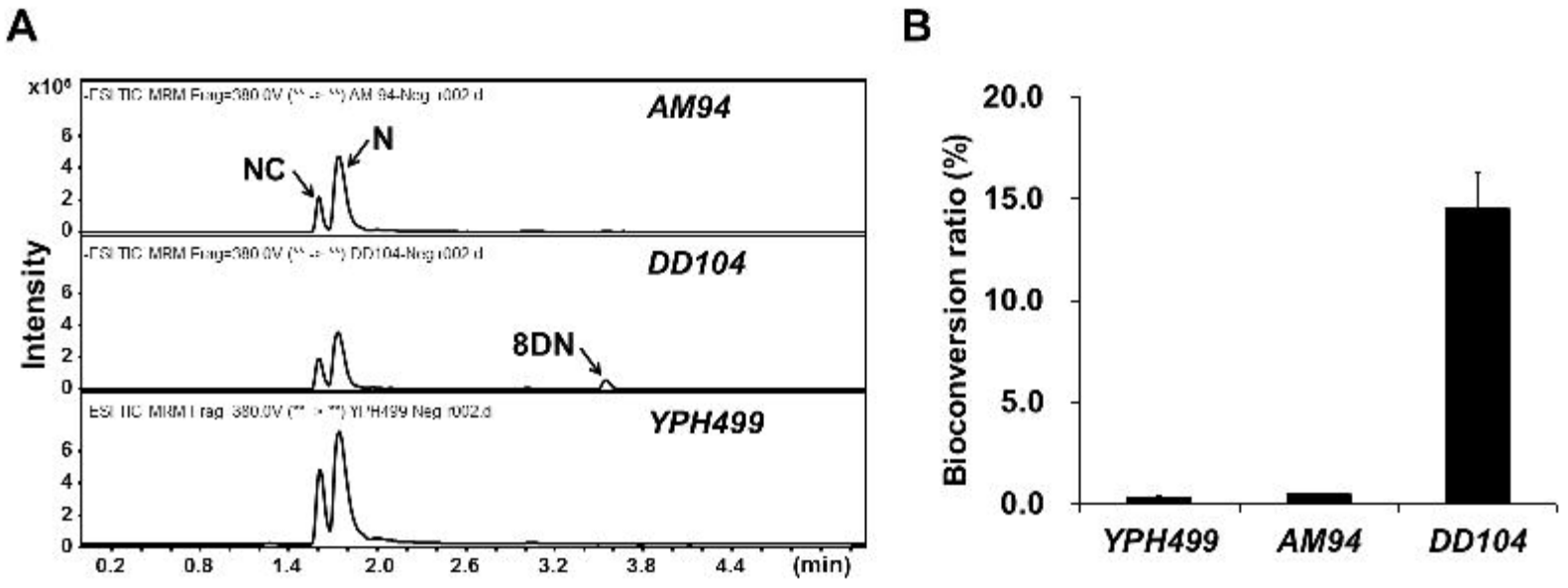

Figure 2. *In vivo* production of 8DN in various yeast strains. (A) Chemical profiling of different yeast strains by LC-ESI-QQQ/MS. 8DN, 8-dimethylallyl naringenin (RT: 3.54 min, MRM transition: *m/z* 339→151); N, naringenin (RT: 1.73 min, MRM mode: *m/z* 271→119); NC, naringenin chalcone (RT: 1.60 min, MRM mode: *m/z* 271→151). (B) Bioconversion ratio of 8DN from the sum of N and NC in different yeast strains. All experiments were performed in triplicate.

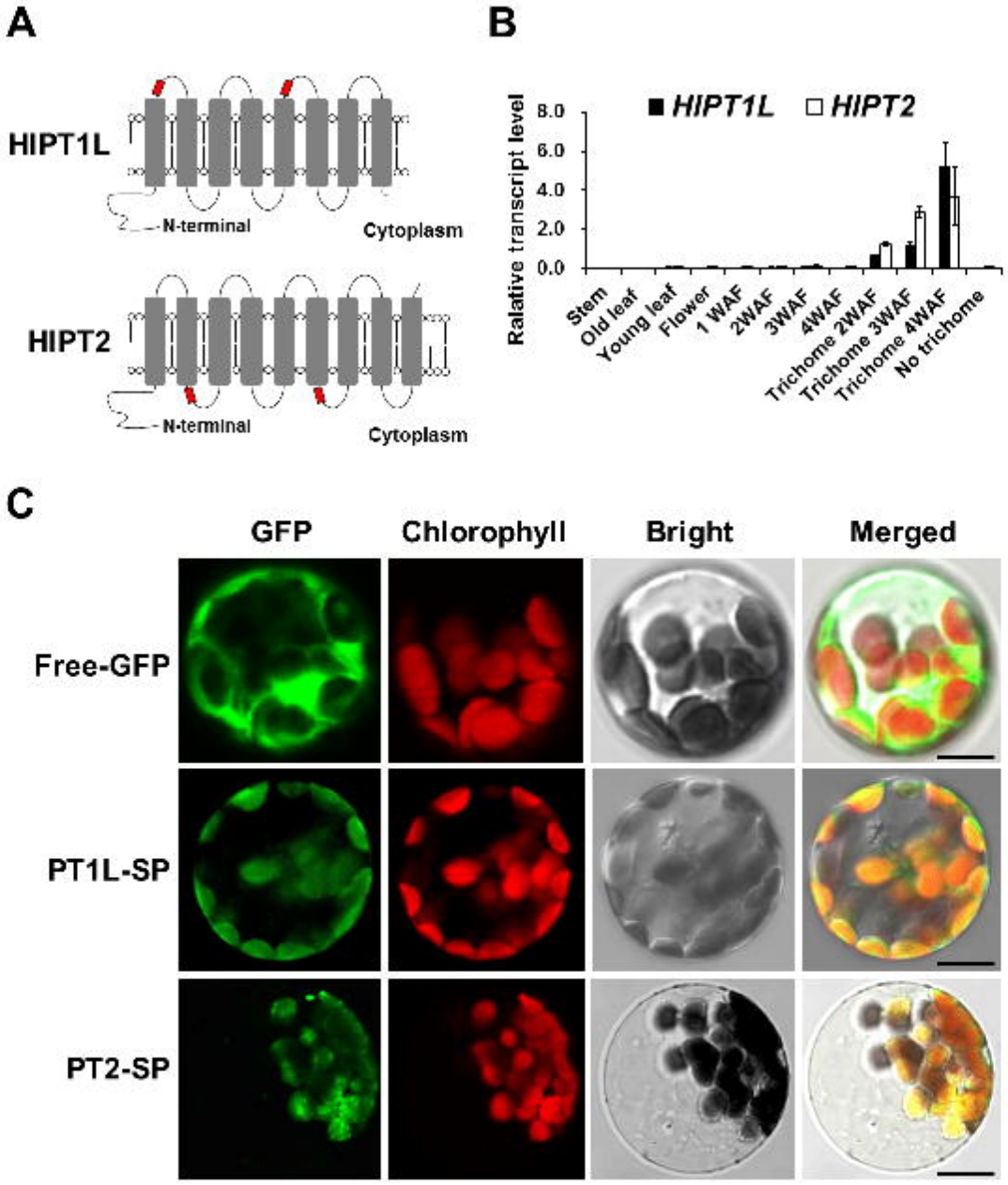

Figure 3. Characterization of HIPT1L and HIPT2 in hop. (A) Membrane topology diagram of HIPT1L and HIPT2. The transmembrane domains and the Asp-rich motifs are highlighted in grey and red, respectively. (B) qRT-PCR analysis of two PT genes in different tissues and different development stages of cones and trichomes. Transcript levels are expressed relative to the GAPDH gene (n = 3). WAF, Weeks after flowering. (C) Subcellular localizations of HIPT1L (the first 86 amino acids at the N terminus) and HIPT2 (the first 83 amino acids at the N terminus) in Arabidopsis leaf-mesophyll protoplasts, as revealed by laser confocal microscopy. Chloroplasts are revealed by red chlorophyll autofluorescence. SP, signal peptide; Scale bars = 10 μm.

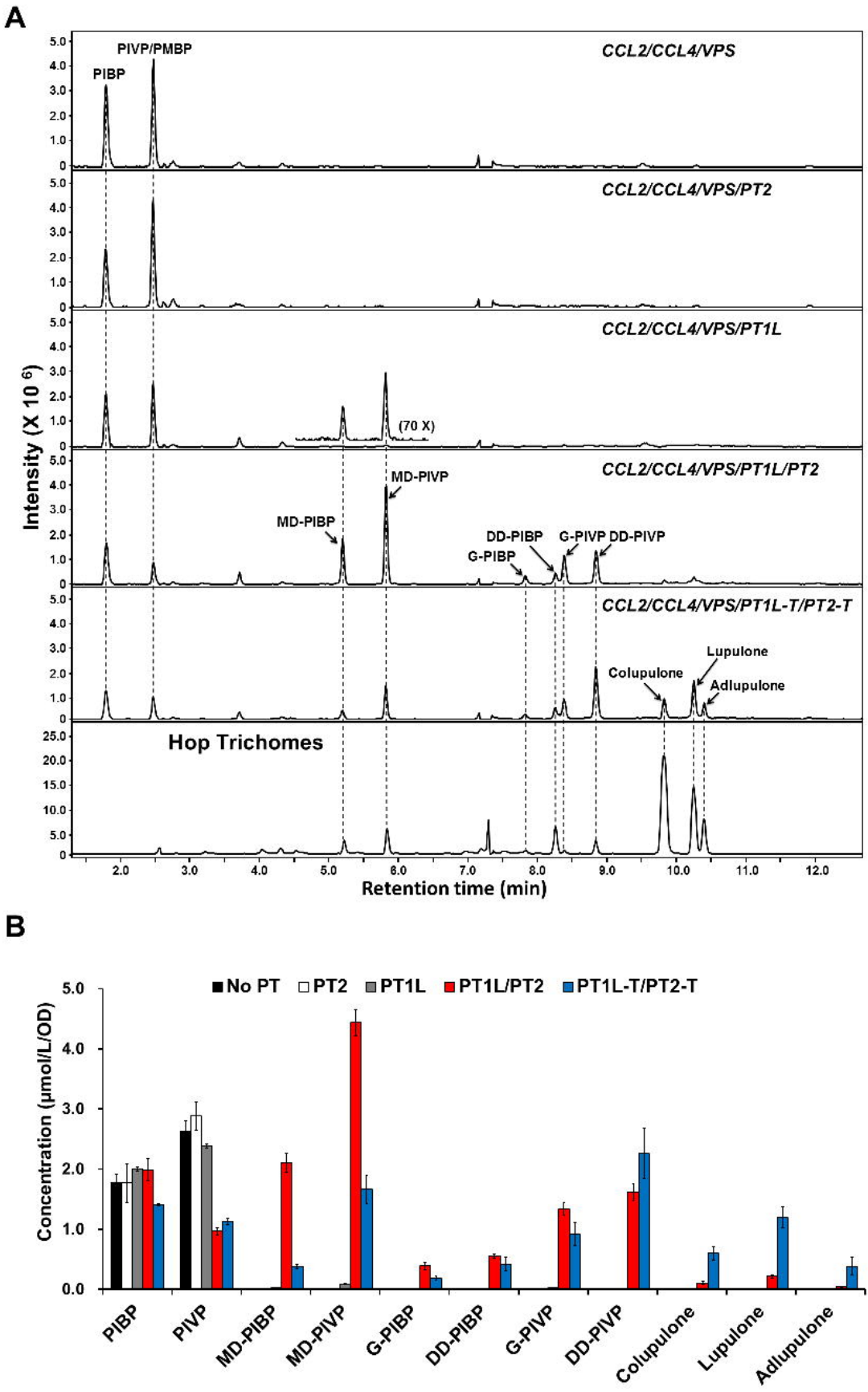

Figure 4. *In vivo* production of prenylated chemicals in yeast cells co-expressing *HlCCL2*, *HlCCL4*, *HlVPS*, and different hop aromatic prenyltransferase genes. (A) Chromatogram of selected ions of m/z 197.0808 for PIBP, m/z 265.1434 for MD-PIBP, m/z 279.1591 for MD-PIVP, m/z 333.206 for DD-PIBP and G-PIBP, m/z 347.2217 for DD-PIVP and G-PIVP, m/z 401.2715 for colupulone, and m/z 415.2863 for lupulone and adlupulone, all with a mass accuracy of ± 10 ppm range. Some regions of these chromatograms have been rescaled to allow easier visualization. (B) Production of different chemicals by yeast strains harboring no *PT* gene (control), *PT1L*, *PT2*, or *PT1L/PT2* (the combination of truncated *HlPT1L* and *HlPT2*). Data are means ± SD for at least three independent clones. See the detailed information for the abbreviations of chemicals in the text. All PT genes used in this experiment were Arabidopsis codon-optimized sequences.

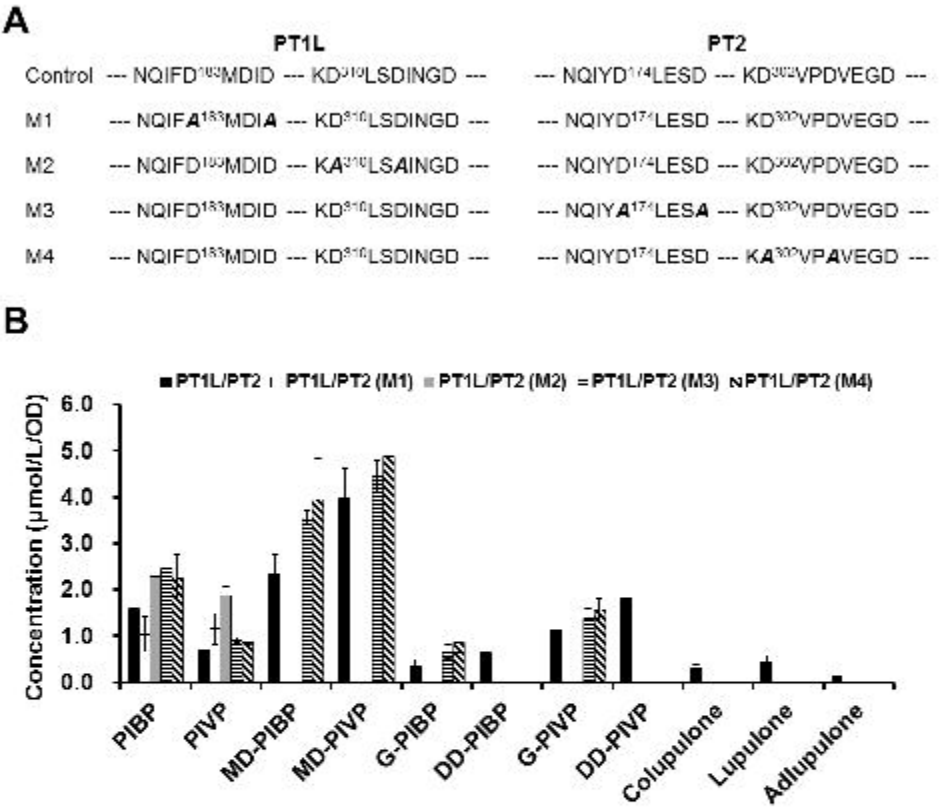

Figure 5. Effects of the Asp-rich motif on bitter acid production in engineered yeast strains. (A) Sequence comparisons of wild-type (control) and mutant PT1L/PT2. Only the Asp-rich motifs are shown, and the mutated amino acids are in bold and italics. (B) Production of different compounds by yeast strains harboring wild-type and mutated *PT1L/PT2* pairs. Data are means + SD for at least three independent clones. All PT genes used in this experiment were Arabidopsis codon-optimized sequences.

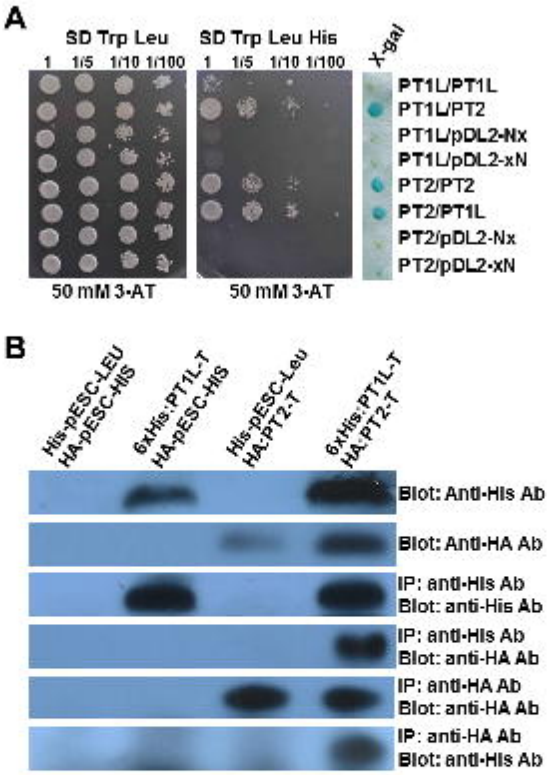

FIgure 6. Direct interaction between PT1L and PT2 in yeast membranes. (A) Split-ubiquitin assays for PT1L and PT2 protein interactions. The different transformed yeast cells were serially diluted and spotted onto growth media (SD/ Trp$^-$/Leu$^-$) and selection media (SD/ Trp /Leu /His), both supplemented with 50 mM 3-AT (3-amino-1,2,4-triazole). The positive interaction between PT1L and PT2 was confirmed by filter assay for detection of X-galactosidase activity. (B) Reciprocal co-immunoprecipitation of His-tagged truncated PT1L and HA-tagged truncated PT2 in yeast cells using HA- and His- antibodies. Total protein extracts from transformed yeast strains harboring truncated *PT1L-At* and *PT2-At* alone or together, were incubated with anti-His or anti-HA antibodies, and the immunoprecipitates were separated by SDS-PAGE and subjected to immunoblot analysis using anti-HA or anti-His antibodies. The His-pESC-LEU and HA-pESC-HIS were used as negative controls. Ab, antibody.